

*Research Article*

## CYCLE TESTS AND STRUCTURE REPAIR OF BRIDGE PIER MODELS

**Innino Justitiannisa<sup>1\*)</sup> and Riawan Gunadi<sup>1)</sup>**<sup>1)</sup>Department of Civil Engineering, Politeknik Negeri Bandung, Bandung, Indonesia

Received: 15 June 2023, Accepted: 3 November 2023, Published: 24 February 2024

### Abstract

This research was conducted in anticipation of the risk of fatal damage to the structure due to the earthquake. In this study, experiments were carried out on the test object in the form of a bridge pillar model, which consisted of 2 test steps. The cyclic test is in the form of a pier bridge model and is continued in step 2 in the form of repairs with grouting and carbon wrapping materials as well as conducting another cyclic test to evaluate the performance of the repair materials used. This study uses the pier model, which consists of two test objects, namely a column with dimensions of 0.25x0.25x1.68 meters and a column cap of 1.20x0.55x0.36 meters. This test provides a constant axial load of 0.2 fc'. Ag and a cyclic lateral load. Phase 1 testing was carried out until the drift ratio was 3.5%. The achieved lateral peak strength is 8,606 tonf with a drift ratio of 2.20%. Lateral strength experienced a decrease in peak lateral strength of 86.93%. The damage is dominated by shear cracks which are characterized by the number of cracks with a diagonal pattern. Structural performance analysis was carried out according to ACI 374.1-05. The results of the theoretical analysis of the peak strength of the pier model were 15.2144 tonnes in the tensile direction, while the experimental ones were 8.606 in the pushing direction and -7.812 in the pulling direction.

**Key Words:** axial load, cyclic test, lateral load, pier, peak strength.

### 1. INTRODUCTION

Indonesia is one of the countries that has a fairly high rate of earthquake occurrence. Earthquakes with a fairly large and damaging scale occurred twenty times in 2017 and twenty-three times in 2018 (BMKG, 2019) An earthquake with a fairly large scale resulted in damage, one of which was the damage that occurred to the bridge pier. Damage to the bridge pier occurs at the end of the base of the pier which is usually in the form of cracks or spalling (Wu & Pantelides, 2017).

Structures that are damaged cause a decrease in the performance of the structure so it must be overcome by carrying out repairs to restore the performance of the structure. Structural repairs that can be applied to damaged structures include RC jackets, fiber-reinforced polymer (FRP), grouting, patching, and wrapping (Wu & Pantelides, 2017). This study made repairs using grouting and wrapping materials. Grouting is a process of inserting cement paste into the cracks in cracked concrete (Udiana, 2013). According to (Paksa, 2020), carbon fiber is one of the composite materials. Carbon fiber composite is a type of composite material that uses carbon fiber as one of its constituents. Composite materials have two main components, matrix and reinforcement material. Carbon fiber serves as a reinforcing material in carbon fiber composites. As

for the matrix, polymer resins such as epoxy are used which function to bind reinforcing materials.

The grouting or repairing process is an attempt to insert cement paste into the cracks in the concrete. The use of grouting or retrofitting is usually used for buildings that have suffered post-earthquake damage (T.Jiang et al, 2016).

Cyclic load is a repeated load received by the structure. To assess the behavior of concrete structures due to cyclic loading, the hysteresis loop is an important thing to observe in the cyclic test (Achmad et al, 2020). Based on SNI 7834:2012, the test object must be loaded by a series of cyclic control circuits that represent the expected drift ratio at the connection during an earthquake. The cyclic test was carried out with three full cycles with a gradually increasing drift ratio (*Standar Nasional Indonesia*, 2012).

The strength of the structure is affected by the cracks that occur in the specimen. Before cracks occur, the strength of the structure is fully carried by the concrete and reinforcement. The greater the load borne by the structure, the greater the cracks resulting in a decrease in the strength of the structure. The greater the initial load in the cyclic experiment, the greater the peak load achieved, the greater the decrease in peak load, the smaller the energy dissipation, and the heavier the level of damage (Raja Marpaung et al., 2014).

Experimental tests in the form of cyclic tests on columns using 17 MPa concrete quality and CFRP as reinforcement showed the results that using CFRP could increase the peak load capacity by 20% in the push direction and 21% in the pull direction with an increase in energy dissipation of 216% (Kurniawan & Oesman, 2021).

A cyclic test of intact portals which were then repaired. The repaired specimens showed a higher lateral load capacity of 5.5% compared to the intact specimens. Intact and repaired portals experience yielding of reinforcement at relatively the same load level, but repaired portals experience greater lateral displacement/drift compared to intact portals. The magnitude of the cumulative energy dissipation in intact portals is greater than in repair portals. This shows that the intact portal still provides better performance than the repair portal (Mariana et al., 2014).

Cyclic testing on reinforced concrete columns using FRP external confinement as reinforcement. The FRP used was in the form of CFRP and GFRP where the two FRPs provided a more effective restraint effect than columns without FRP which showed the effectiveness of the restraints increased by 1.45 and 1.58. Meanwhile for single-layer CFRP columns showed an increase in  $P_n$  and  $M_n$  against columns without FRP by 134.66% and 20.54% and against GFRP columns by 8.62% and 4.65%. However, carbon fiber is indicated to provide a better increase in strength compared to glass fiber type external restraint columns (Achmad et al, 2013).

(Widiarsa & Hadi, 2013), shows that a column using 1 layer of CFRP wrapped increases the strength of the column in bearing the load by 14.8%. The use of CFRP wrapped improves column performance by slowing down the cracking of concrete. (Del Zoppo et al., 2017), shows that columns with limited CFRP can prevent brittle failure and increase deformation capacity by 60.4%.

(Ghate et al., 2015), tested a full scale column with FRP as reinforcement in a cyclic test which had an average peak lateral strength of 63.23 kN at a drift ratio of 1.5% with a displacement of 30.1 mm followed by a decrease in lateral strength when next cycle. Concrete is damaged and buckling occurs in the longitudinal reinforcement when the drift ratio is 4% and 7%.

(Rahman et al., 2015), conducted experimental cyclic tests on bridge piers with ultra-high strength concrete capable of achieving a drift ratio of 5.80% with a displacement ductility factor of 5.35 on a HRSP-70 test object (Hollow Rectangular Section Pier with an axial load of  $0.075fc'Ag$ ), while the displacement ductility factor of the Hollow Rectangular Section Pier with an axial load of  $0.15fc'Ag$  (HRSP-60) decreased to 4.58 at a drift ratio

of 3.50%. HRSP-70 is able to accommodate stiffness degradation from the first melting state to the boundary conditions up to 82.99%, but in HRSP-60 it is only about 77.86%. energy dissipation on HRSP-60 decreased by 39.46% after the compressive axial force was increased by 50%.

(Thermou et al., 2018), conducting RC column tests using steel reinforced grout (SRG) jacketing showed that SRG jacketing can substantially increase the structural response of reinforced elements by increasing deformation capacity and preventing structural failure modes. The reinforced columns experienced bending failure and achieved an average drift ratio of 4.5% showing a gradual decrease in strength. SRG jacketing column prevents brittle failure.

(Megasari et al., 2015), tested reinforced concrete columns with carbon fiber jacketing shear reinforcement for column shear strength due to constant axial loads and cyclic lateral loads which showed that the reinforcement columns experienced an increase in lateral load capacity of 309.743% compared to comparison columns. The reinforcement column is more ductile with an increase in ductility of 23.871%. The damage condition on the surface of the reinforced column is better than that of the comparison column, so that the reinforcement column with the carbon fiber jacket method can reduce or overcome cracks and increase the shear strength of the column.

(Parmo et al., 2013), repaired columns subjected to cyclic loads using GFRP. Testing is done with

the constant axial load is 748 kN and the cyclic lateral load uses displacement control to simulate earthquake loads. This test shows an increase in column lateral capacity of 43.96%. GFRP is ductile which is indicated by an increase in deformation of 129.14%.

Therefore, this research will be carried out to repair the damaged bridge pier model due to cyclic loads. The bridge pier model will be repaired using grouting and wrapping materials. The cracked pier model will be repaired with a grouting agent to reduce the permeability coefficient and increase the compressive strength. The wrapping material used is a carbon wrap which aims to increase the shear capacity. However, this discussion will only explain the results of the first step of the cyclic test on the intact bridge pier model.

## 2. METHOD

This research was conducted on one test object which is a bridge pier model. The pier model uses polymer concrete with a mixture of Styrene-Butadiene Rubber (SBR) materials. The pier model consists of 2 parts in the form of a column with dimensions of 0.25x0.25x1.68 meters and a stamp

column of 1.20x0.55x0.36 meters. The test object specifications will use FC'30 concrete, which is the average compression of cylindrical concrete strength test at 28 days of age and  $f_y$  400 MPa deform reinforcement. The results of the reinforcement tensile test are shown in Table 1. Figure 1 shows the specifications of the pier model as follows.

Table 1. Result of Reinforcement Tensile Test

	Diameter (mm)	Yield Stress (MPa)	Fracture (MPa)
(1)	(2)	(3)	(4)
BJTP 24	8	444.37	645.90
BJTD 40	10	748.43	877.47
BJTD 40	16	532.43	684

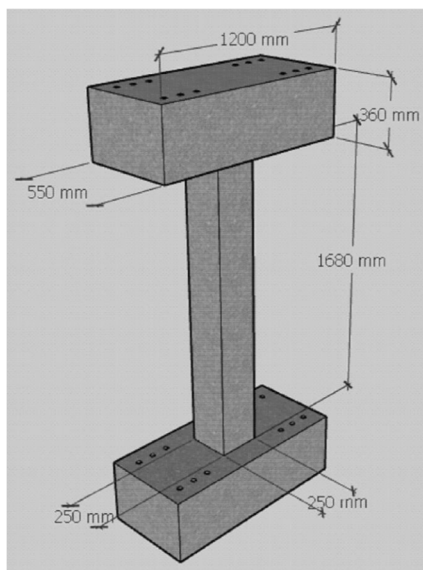


Figure 1. Pier model specifications

The pier model uses longitudinal reinforcement 8D16 and 4D10. The stirrup used with a diameter of Ø8-75 mm and Ø8-125 mm, as indicated in Figure 2. On the bridge pier model, two strain gauges are installed in one direction for lateral loading. Strain gauge instrument installation in the bridge pier model can be seen in Figure 3.

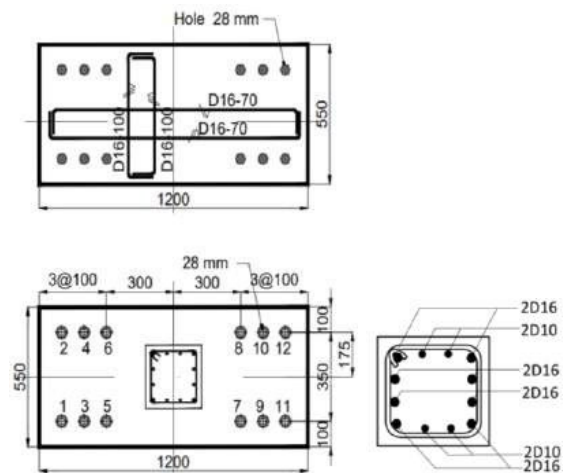
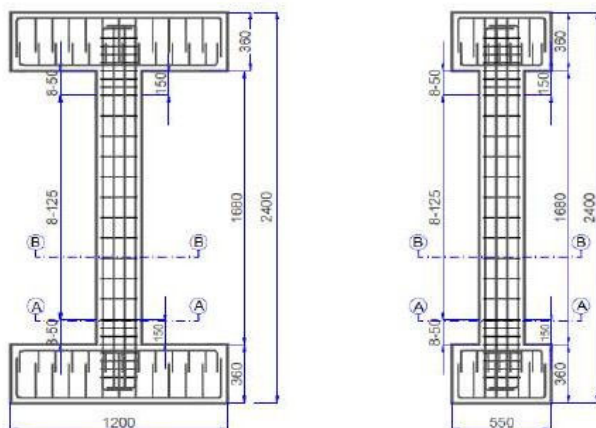


Figure 2. Reinforcement details of the bridge pier model

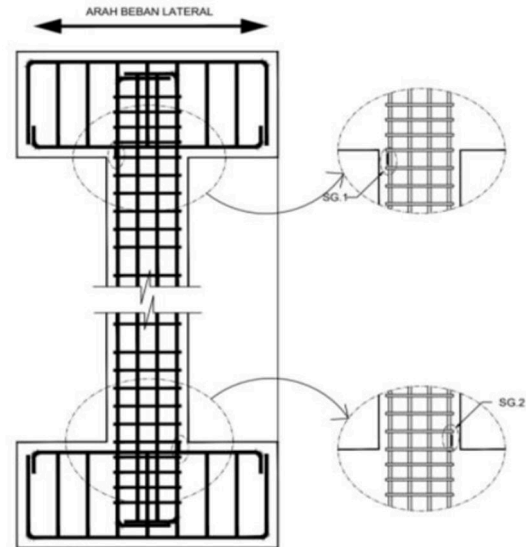


Figure 3. Strain gauge location on bridge pier model

This research consists of two testing steps. Step 1 is cyclic testing on the bridge pier model. Step 2 is in the form of structural repair (using grouting and wrapping materials) and cyclic testing again. The cyclic test was carried out according to ACI-374-1-05. The specimen will be loaded in the form of static axial force and constant lateral force until the pier model collapses. The pier model is given a constant axial load of  $0.2f_c'Ag$  and cyclic lateral load with a displacement control method.

When the cyclic test is to be carried out, the pier model is mounted on the loading frame and then a Linear Variable Displacement is installed to identify damage at several points when a lateral load is applied to the pier model. This test provides a load in the form of alternating direction deviation. There are 3 cycles for each deviation with an increase in the given deviation 0.25 – 0.5 times greater than the previous deviation. The cyclic test is terminated when the specimen is at a load level of approximately 80% of the peak load. The loading pattern in this test can be seen in Figure 4 and in Figure 5 can be seen the tool settings, test illustrations, and LVDT locations during cyclic testing.

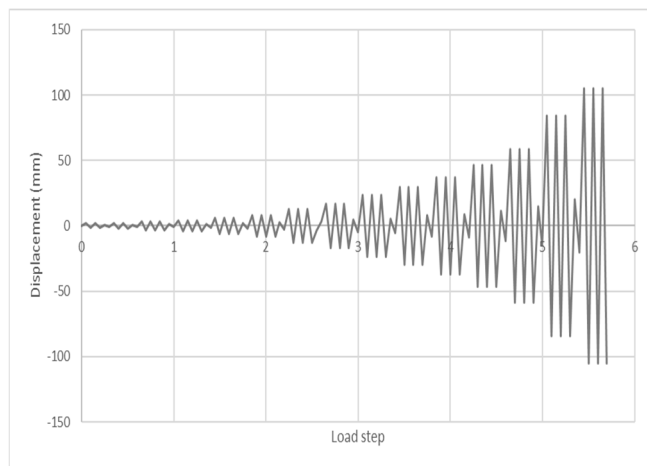


Figure 4. Lateral loading pattern

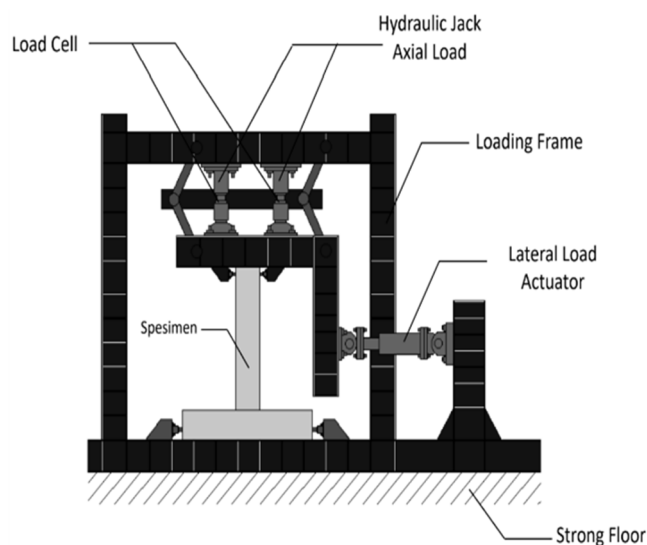


Figure 5. Pier model illustration

### 3. RESULTS AND DISCUSSION

This test was carried out experimentally on a bridge pier model. The discussion that will be displayed is the results of cyclic testing on the pier model step 1, cyclic testing step 2 (repairs with grouting and wrapping materials), and theory, then

the results will be compared. Theoretical analysis will be calculated for intact (theoretical) and cracked pier model conditions. The theoretical results compared with experimental results are load-displacement, initial stiffness, and peak strength. The results of step 1 of the experiment showed a decrease in structural performance due to damage to the pier model when cyclic loads were applied. The results of step 1 of testing will be a comparison for step 2 testing using the same test object but previously repaired with repair materials. The repair materials used are wrapping and grouting. Cyclic test results will be analyzed based on ACI 374.1-05. ACI 374.1-05 is used for building reception systems but in this research, it is used for bridges so ACI 374.1-05 only takes parameters in it which are useful for analyzing and comparing the results of cyclic tests on step 1 and step 2. Analysis and discussion of the performance of the first step of the pier model are explained as follows.

#### Relationship of Lateral Load and Displacement

The test results at step 1 and step 2 showed that the relationship between lateral load and displacement was displayed in the form of a hysteresis curve as shown in Figure 6 and Figure 7 below.

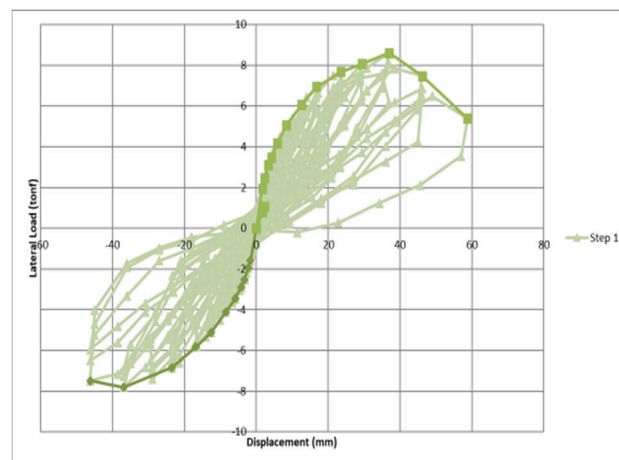


Figure 6. Hysteresis curves in the first step

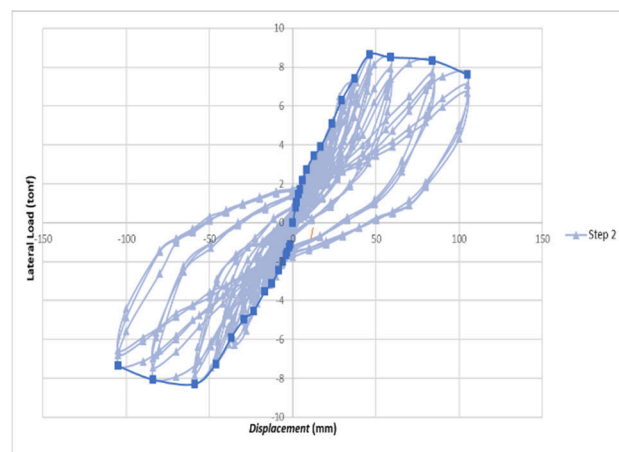


Figure 7. Hysteresis curves in the second step

Figure 6 shows in the first step that when the pier model is given a thrust load, the load increases significantly in line with the increase in displacement that occurs up to a drift ratio of 2.20%. After that, the curve decreased to a drift ratio of 3.50%, as was the case when a tensile load was applied.

Figure 7 shows the results of cyclic testing in step 2 where testing was carried out until the drift reached 6.25% for push and pull direction. The overall hysteresis curve obtained shows a good picture of behavior because there is no decrease in stiffness and significant strength during loading at any drift ratio. The second stage of testing experienced quite large and still displacement able to survive without causing further damage in several loading cycles.

Analysis of the load-displacement relationship carried out theoretically with a given axial load of 30 tonf and a nominal moment of 66 kN.m produces a lateral load of 8.0121 tonf in the push and pull directions. The theoretical calculated lateral load is plotted on the spine curve which can be seen in Figure 8 so that the displacement in the intact (theoretical) condition is 5.59 mm in the pushing direction and -2.54 mm in the pulling direction. In cracked conditions, the displacement in the pushing direction shows a result of 6.42 mm and -4.87 mm in the pulling direction. while the experimental results in step 1 with a lateral load of 8.0121 tonf showed a displacement of 11.50 mm in the pushing direction and -10.33 in the pulling direction. The experimental results in step 2 with a lateral load of 8.0121 tonf showed a displacement of 18.83 mm in the pushing direction and -20.39 in the pulling direction. This shows that the displacement at the lateral load of 8.0121 tonf is greater than the results of the displacement when intact and cracked (theoretical). The results of theoretical and experimental calculations of the load - displacement relationship can be seen in Table 2.

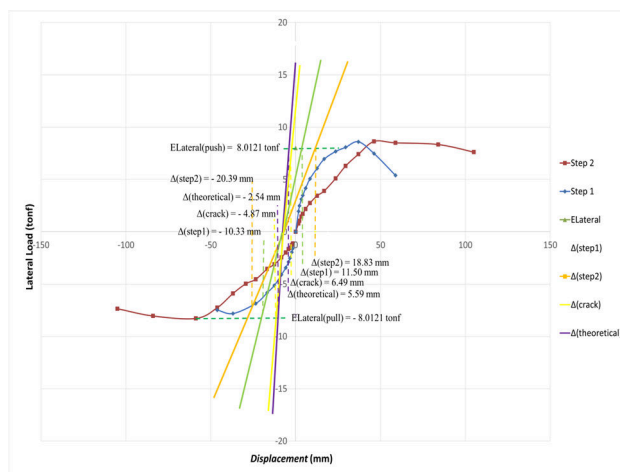


Figure 8. Backbone Curve in the first and second steps

Table 2. Results of theoretical and experimental calculations of the load-displacement relationship

	Loading Condition	Lateral Load (tonf)	Displacement (mm)
(1)	(2)	(3)	(4)
Step I	Push (+)	8,0121	11.50
	Pull (-)	-8,0121	-10.33
Step II	Push (+)	8,0121	18.83
	Pull (-)	-8,0121	-20.39
Crack	Push (+)	8,0121	6.42
	Pull (-)	-8,0121	-4,87
Intact (Theoretical)	Push (+)	8,0121	5.59
	Pull (-)	-8,0121	-2.54

**Stiffness**

The initial stiffness is the ratio between the force and the displacement that occurs at the initial applied lateral load which can be described as the slope in the displacement interval of +0.35% to -0.35%. The test results on the pier model in the first step of the experiment had a lower initial stiffness compared to theoretical calculations both in intact condition and when cracked. Theoretical and experimental results can be seen in Table 3 and Figure 9.

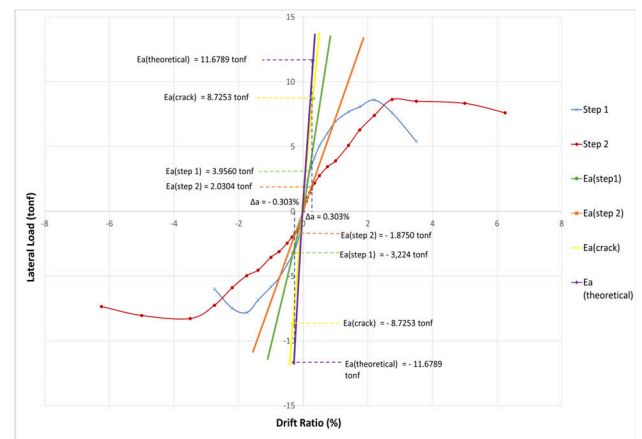


Figure 9. Initial Stiffness in the first and second steps

Table 3. The results of the initial stiffness calculation

	Loading Condition	Drift Ratio (%)	$\Delta_a$ (mm)	$E_a$ (tonf)	$K_o$ (tonf/mm)
(1)	(2)	(4)	(5)	(6)	(7) = (6)/(5)
Step I	Push (+)	0.303%	5.50	3.9580	0.7196
	Pull (-)	0.303%	5.50	3.2240	0.5862
Step II	Push (+)	0.303%	5.50	2.030	0.3693
	Pull (-)	0.303%	5.50	1.875	0.3408
Crack	Push (+)	0.303%	5.50	11,6789	2,1234
	Pull (-)	0.303%	5.50	11,6789	2,1234
Intact (Theoretical)	Push (+)	0.303%	5.50	8,7253	1,5864
	Pull (-)	0.303%	5.50	-8,7253	1,5864

Table 3 shows a drift ratio of 0.303% with a displacement of 5.50 mm giving the initial stiffness results calculated theoretically in the intact (theoretical) condition of 2.1234 and in the cracked condition of 1.5864 in the push and pull directions.

The experimental results in step 1 show an initial stiffness of 0.7196 in the pushing direction and 0.5862 in the pulling direction. Meanwhile, experimental results in step 2 show an initial stiffness of 0.3693 in the pushing direction and 0.3408 in the pulling direction.

Stiffness degradation describes a decrease in structural stiffness during loading and reverses loading. Stiffness degradation is calculated according to ACI 374.1-05. Stiffness calculations in this study were analyzed at a drift ratio of 2.75% which was used as a tool for calculating stiffness. Stiffness degradation was calculated with reference to Figure 10, Figure 11 and Table 3.

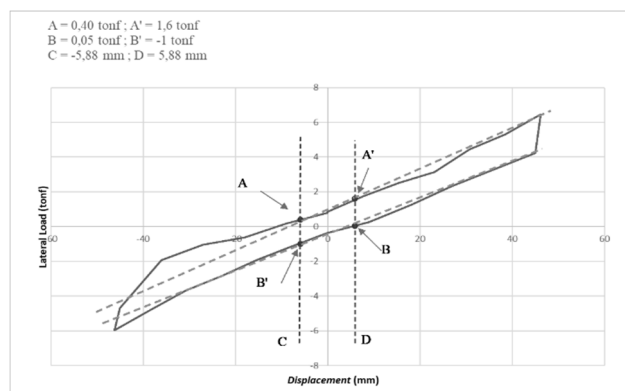


Figure 10. Initial Stiffness in the first step

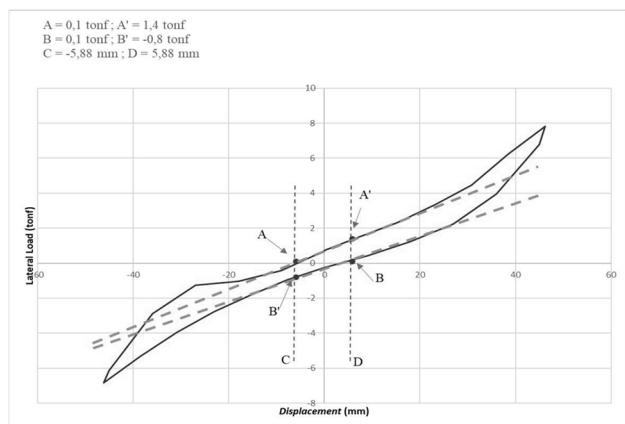


Figure 11. Initial Stiffness in the second step

Table 4. The results of the stiffness degradation calculation

Step	Loading Condition	Initial Stiffness $K_0$ (tonf/mm)	Displacement difference at 0.35% (mm)	Load difference at 0.35% (tonf)	Stiffness at drift ratio 0.35%, $K'$ (tonf/mm)	Ratio $K'/K_0$ (tonf/mm)
(1)	(2)	(3)	(4)	(5)	(6)	(7) = (6)/(3)
I	Push (+)	0.72	11.76	1.20	0.102	14.17
	Pull (-)	0.59	11.76	0.95	0.081	13.69
II	Push (+)	0.37	11.76	1.30	0.110	29.86
	Pull (-)	0.34	11.76	0.70	0.059	17.50

### Peak Strength

Based on the backbone curve in Figure 7, it can be seen that the peak strength obtained in step 1 was 8,606 tonf in the pushing direction and 7,812 tonf in the pulling direction and the peak strength in step 2

was 8,640 tonf in the pushing direction and 8,275 tonf in the the pulling direction. Meanwhile, the peak strength from theoretical calculation results shows a result of 15.21144 tonf in the push and pull directions. The theoretical peak load analysis is carried out by determining the strength.

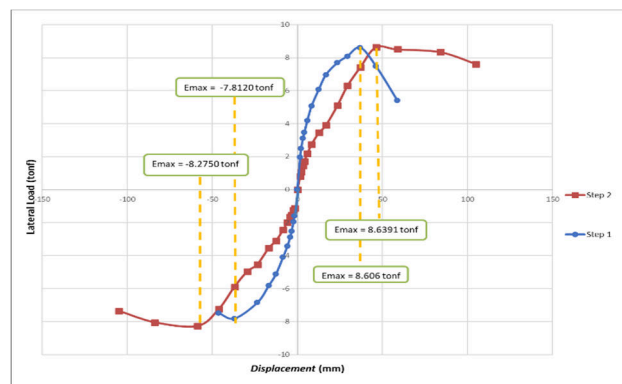


Figure 12. Peak strength in the first and second steps

### Deformation Capacity

According to ACI 374.1-05, the deformation capacity can be calculated in conditions where the lateral load is stopped during softening conditions and should not be less than 75%  $E_{max}$  in the same load direction and the results of the analysis are presented in Figure 8 and Table 3.

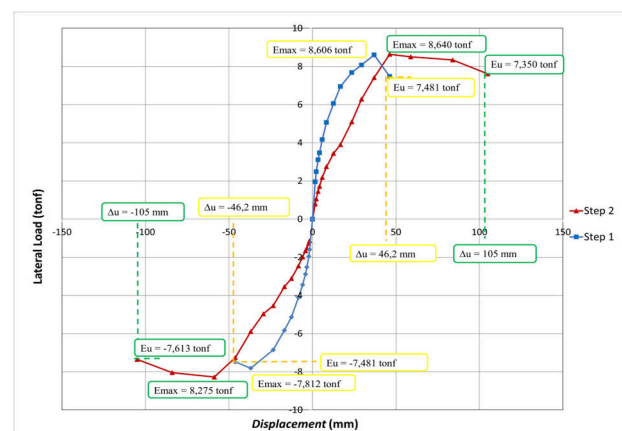


Figure 13. Deformation capacity in the first and second steps

Table 5. The results of the deformation capacity calculation

Step	Maximum Push (+)	Maximum Pull (-)	Maximum Load	$E_u/E_{max} \geq 0.75$
(1)	(2)	(3)	(4)	(5)
I	$E_u$ (tonf)	$\Delta u$ (mm)	$E_u$ (tonf)	$\Delta u$ (mm)
	8.626	39.5	7.481	46.2
II	$E_u$ (tonf)	$\Delta u$ (mm)	$E_u$ (tonf)	$\Delta u$ (mm)
	8.294	87.1	7.944	88.0

### Energy Dissipation

The total energy dissipation can be calculated as the sum of the areas (hysteresis loops) of the third cycle for each drift ratio. The area of the circle is

calculated based on the difference in magnitude the displacement that occurs is multiplied by its magnitude lateral load. The energy dissipation is described as the area of the parallelogram ABCD. The results of the energy dissipation calculation for the first step of testing are presented in Table 6, Figure 14, and Figure 15.

increases and approaches the maximum load, the cracks increase but are still very fine, but after the load reaches the maximum, the pier model collapse and the concrete cover begins to peel off (cover spalling). The damage that occurred in the first step can be seen in Figure 16.

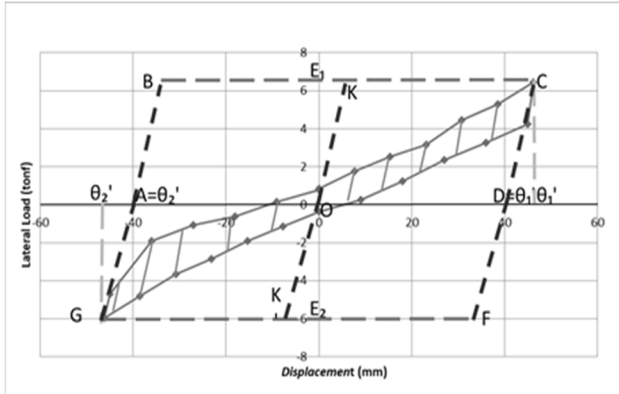


Figure 14. Energy dissipation in the first step

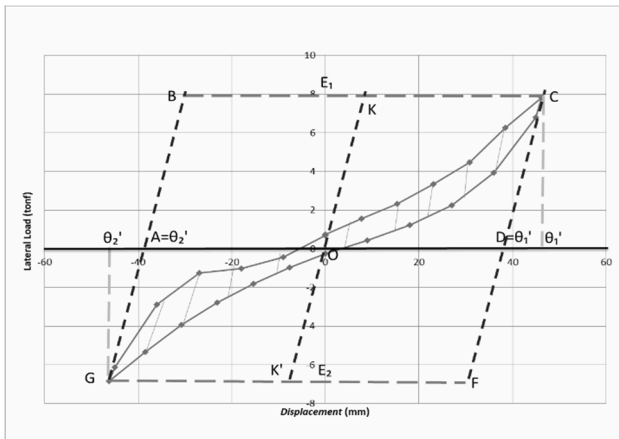


Figure 15. Energy dissipation in the second step

Table 6. The results of the energy dissipation calculation

Step	The area of the shaded region (tonf.mm)	The area is limited by ABCD and DFGA (tonf.mm)	Relative energy dissipation ratio, $\beta$
(1)	(2)	(3)	(4) = (2)/(3)
I	205.0015	1146.9150	17.87
II	204.0915	1354.8890	15.06

### Damage Pattern

In the first step, the lateral load of the pier model is relatively small so that cracks do not occur. However, when the lateral load increases, cracks begin to appear. The first cracks in the first step of testing occurred at a drift ratio of 0.20% with microcracks appearing at the upper and lower ends of the pier model. This crack is dominated by a shear crack that starts from the starboard surface and increases all over the side of the pier model. Cracks experience addition or widening. When the load



Figure 16. Damage pattern in the first step

In the second step of testing the reinforcement has exceeded the yield so that the performance of the reinforcement in response to tension decreases and begins to be replaced by carbon wrap. From the results of observations of the second stage of testing, it shows A tear in the carbon wrap with a bending pattern (longitudinal direction) on the part bottom of the pier. The tear occurred first at a drift ratio of 1%. This shows that carbon wrap is starting to play a role so the shear capacity increases. The tear increases with the rise given load. Elongation or widening of the tear that occurs in the second test when the load increases close to the load maximum. When the maximum load is 8,640 tonf. Damage incurred the second step of testing was dominated by damage due to bending which can be seen in Figure 17.

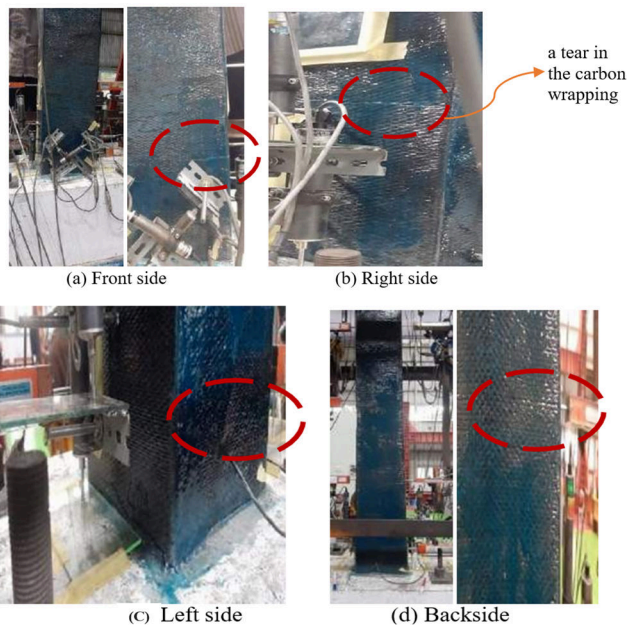
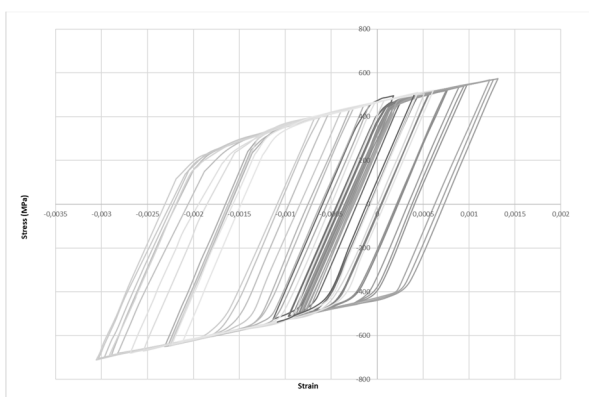


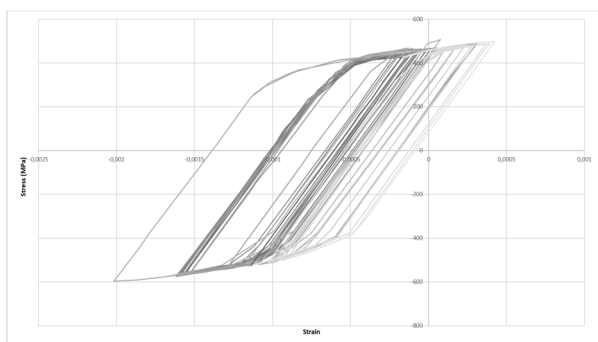
Figure 17. Damage pattern in the second step

### Cyclic Stress-Strain of Reinforcement

The cyclic stress-strain in the first step of test reinforcement was obtained from modeling with the Menegotto-Pinto method. The results of the cyclic stress-strain analysis of the reinforcement are shown in Figure 10. Figures 10a and 10b show the results of the analysis based on the strain identification of the SGT1 and SGT2 strain gauges, respectively, attached to the D16 reinforcement at the top end and at the bottom end of the pier.



(a) Stress-strain reading (SGT-1) on first-step cyclic reinforcement



(b) Stress-strain reading (SGT-2) on first-step cyclic reinforcement

Figure 18. Cyclic stress-strain readings of reinforcement

Figure 18 shows the results of the stress-strain during the yield (elastic) condition at the start of loading which is read at SGT 1 in the push direction with stress of 545.939311 Mpa and a strain of 0.000180288 when the drift ratio is 0.10% with a lateral load of 1.95 tonf and the strain stress read by SGT 2 in the push direction with the stress of 542.3416327 Mpa and a strain of 0.000176998 when the drift ratio is 0.10% with a push lateral load of 1.557 tonf. The maximum strain obtained from the results of the first step of testing for the push direction in the drift direction is 0.50% and the pull direction is 1.75% which is read on SGT 1 and SGT 2. The maximum strain read by SGT in the push direction is 574.01736 MPa and strain of 0.001313 and the maximum stress in the pull direction of -711.0730 MPa and strain -0.003059. The results of SGT 2 show that the maximum stress in the push direction is 496.6689 MPa and the strain is -0.000424 and in the pull direction the stress is -595.9668 MPa and the strain is -0.0020180.

### 4. CONCLUSION

Based on the results of step 1 and step 2 tests carried out, it can be seen that the bridge pier model shows nonlinear behavior when the initial stiffness is lost as the lateral load increases. The initial stiffness results of the step 2 pier model decreased from step 1 is 51.304% in the push direction and 58.145% in the pull direction.

There was an increase in stiffness degradation in step 2 by 211.160% in the push direction and 126.725% in the pull direction compared to step 1. The experimental results showed that the ability to accept the maximum load in step 2 was greater than the step 2 by 100.395% in the push direction and 105.932% in the pull direction.

The deformation capacity describes the behavior of a structure once it reaches its ultimate limit. The large deformation capacity is caused by the loss of structural strength when it reaches the ultimate limit so that the concrete collapses. The deformation capacity of step 2 increased by 220.506% in the push direction and 190.476% in the pull direction compared to testing step 1. In this test, the deformation capacity is taken as 96%  $E_{max}$ . The energy dissipation in this bridge pier model during step 2 is lower than in step 1 by 84.274%.

The results of the stress-strain in the first step of SGT 1 show that the maximum stress in the pushing direction is 574.01736 MPa and the strain is 0.001313 at a drift ratio of 0.50% and the maximum stress in the pulling direction is -711.0730 MPa and the strain is -0.003059 at a deviation ratio of 1.75%. The results of SGT 2 in the first step of testing showed that the maximum stress in the thrust direction was 496.6689 MPa and the strain was -

0.000424 at a drift ratio of 0.50%. and -595.9668 MPa at tensile stress and -0.0020180 at strain with a drift ratio of 1.75%. However, the reinforcement experienced the first yield at a drift ratio of 0.10% with a stress of 545.939311 Mpa and a strain of 0.000180288 which was read at SGT 1 and at SGT 2 it was read that the reinforcement had yielded at a drift of 0.10% with a stress of 542.3416327 Mpa and Strain 0.000176998.

The pier model suffered damage in step 1 which was dominated by shear cracks (diagonal/oblique cracks) which started from the edge of the pier and spread to all sides and along the height of the pier causing cracks in the pier which exceeded the thickness of the concrete layer. The crack pattern is cracked at the edge of the pier and spreads wider towards the middle of the span until cover spalling occurs. Repair with grouting and wrapping materials in step 2 is possible prevent the expansion of shear cracks due to previous loading and prevent the appearance of new shear cracks thereby forming a crack pattern development of flexural cracks with the resulting crack patterns after the bridge pier model was repaired.

## ACKNOWLEDGEMENTS

This research was sponsored by the Bandung State Polytechnic through the Postgraduate Research (PPS) scheme at the Research and Community Service Unit (UPPM) and PT Hissan Indonesia which helped financially. In addition, PT Hissan Indonesia assisted in procuring repair materials in the form of grouting and carbon wrapping materials. We thank the Bandung State Polytechnic and PT. Hissan Indonesia has supported this research so that the writer can complete it properly.

## REFERENCES

- Achmad, K., Smd, A., & Tavio, D. (n.d.). *Metode Eksperimental Struktur Kolom Beton Bertulang Tahan Gempa Menggunakan CFRP Sebagai Eksternal Confinement* (Vol. 1, Issue 1).
- BMKG. (2019). *Katalog Gempabumi Signifikan dan Merusak 1821-2018* (T. Prasetya (ed.)).
- Del Zoppo, M., Di Ludovico, M., Balsamo, A., & Prota, A. (2017). Behavior of CFRP confined RC columns under axial load and uniaxial cyclic lateral loading. *COMPADYN 2017 - Proceedings of the 6th International Conference on Computational Methods in Structural Dynamics and Earthquake Engineering*, 2, 2753–2764. <https://doi.org/10.7712/120117.5604.16923>
- Eksperimental, P., Siklik, P., Persegi, P., Jembatan, B., Beton, D., Ultra, B., Mohammad, T., Rahman, J., Budiono, B., Surono, A., & Sipil, T. (2015). 4. Mohammad Junaedy R, dkk Vol.22 No.2 Hal 99-114.pub. *Agustus*, 22(2).
- Ghatte, H. F., Demir, C., Ilki, A., & Ghatte, H. F. (2015). *Seismic performance of full-scale FRP retrofitted substandard rectangular rc columns loaded in the weak direction*. <https://www.researchgate.net/publication/278966147>

- Katalog-Gempabumi-Signifikan-dan-Merusak-1821-2018*. (n.d.).
- Kekuatan, P., Daktilitas, D., Beton Bertulang, K., Mendapat, Y., Gempa, B., Agoes, P., & Tavio, S. M. D. (2013). *Menggunakan Glass Fiber Reinforced Polymer* (Vol. 36, Issue 1).
- Kurniawan, P., & Oesman, M. (2021). *The Behavior of Low-Strength Reinforced Concrete Column Strengthened with Carbon Fiber Reinforced Polymer Subjected to Cyclic Lateral Load*.
- Mariana, R., Badriah, S., & Imran, I. (2014). Kinerja Struktur Portal Terbuka Beton Bertulang Terhadap Beban Lateral. *Jurnal Teknik Sipil* (Vol. 10).
- Megasari, S. W., Yos, J., Km, S., & -Pekanbaru, R. (2015.). *Perilaku Kolom Beton Bertulang Dengan Perkuatan Geser Carbon Fiber Jacket*.
- Raja Marpaung, P., Suhirkam, D., Flaviana Tilik, L.(2014). Perilaku Struktur Beton Bertulang Akibat Pembebanan Siklik. *PILAR Jurnal Teknik Sipil*, 10(2).
- Standar nasional Indonesia*. (2012). [www.bsn.go.id](http://www.bsn.go.id)
- Thermou, G. E., Hajirasouliha, I., & Papanikolaou, V. K. (2018). *A novel method for seismic retrofitting of substandard RC columns using steel-reinforced grout jacketing*. <https://www.researchgate.net/publication/326462358>
- Udiana, I.M. (2013). Desain Campuran Semen dan Air pada Pekerjaan Grouting Proyek Bendungan/Waduk Nipah Madura-Jawa Timur. *Jurnal Teknik Sipil* 2 (2), 93-104. <https://www.neliti.com/id/publications/142236/desain-campuran-semen-dan-air-pada-pekerjaan-grouting>
- Widiarsa, I. B. R., & Hadi, M. N. S. (2013). Performance of CFRP wrapped square reinforced concrete columns subjected to eccentric loading. *Procedia Engineering*, 54, 365–376. <https://doi.org/10.1016/j.proeng.2013.03.033>
- Wu, R. Y., & Pantelides, C. P. (2017a). Rapid seismic repair of reinforced concrete bridge columns. *ACI Structural Journal*, 114(5), 1339–1350. <https://doi.org/10.14359/51700789>
- Wu, R. Y., & Pantelides, C. P. (2017b). Rapid seismic repair of reinforced concrete bridge columns. *ACI Structural Journal*, 114(5), 1339–1350. <https://doi.org/10.14359/51700789>

